Hemispheric helicity sign rule and its solar cycle dependence

M. Zhang[1]*, J. Hao[1] and C. Y. Wang[2]

[1]*Key Laboratory of Solar Activity, National Astronomical Observatory,*
Chinese Academy of Sciences
[2]*National Center for Space Weather Monitoring and Warning,*
Chinese Meteorological Administration

Abstract. We take two approaches to study whether the hemispheric helicity sign rule is preserved over a whole solar cycle or not. We find that, for global-scale magnetic fields on the photosphere, the hemispheric helicity sign rule is evident in fields up to 60 degrees in latitude and shows no solar-cycle dependent. For active regions observed by SP/Hinode, the hemispheric helicity sign rule is preserved in the ascending phase of solar cycle 24, but not in the descending phase of solar cycle 23.

Keywords : Sun: magnetic topology – Sun: photosphere – sunspots

1. Introduction

Solar magnetic fields are observed to emerge into each hemisphere with a preferred helicity sign: positive in the southern hemisphere and negative in the northern hemisphere. This is the so-called usual hemispheric helicity sign rule and has been observed in solar cycles 21, 22 and 23 using various instruments (e.g. Pevtsov, Canfield & Metcalf 1995, Pevtsov, Canfield & Latushko 2001; Bao & Zhang 1998; Hagino & Sakurai 2004; Zhang 2006). There seems no argument on the existence of this hemispheric helicity sign rule. However, there is an argument on whether this rule is preserved over a whole solar cycle or not.

Bao, Ai & Zhang (2000) first pointed out that current helicity density in their data show an opposite hemispheric preference at the beginning of solar cycle 23. Following

---

*email: zhangmei@bao.ac.cn

them, several studies (Hagino & Sakurai 2005, Tiwari, Venkatakrishnan & Sankara-subramanian 2009, Zhang et al. 2010) have reported that the hemispheric helicity sign rule may not be satisfied in the solar minimum phase. Choudhuri, Chatterjee & Nandy (2004) developed a model that predicts deviations from the usual hemispheric rule at the beginning of a solar cycle, result of which has been reproduced in a more simple but parameter-tunable dynamo model (Xu et al. 2009). However, Pevtsov, Canfield & Latushko (2001) argued that the usual hemispheric helicity sign rule still holds for the first four years of solar cycle 23 although by nature it is a weak rule with significant scatter. In Pevtsov et al. (2008) authors further concluded that "the notion that the hemispheric helicity rule changes sign in some phases of solar cycle is not supported at a high level of significance".

In this talk we present our recent works on addressing this question, that is, whether the hemispheric helicity sign rule is preserved over a whole solar cycle or not. We take two different approaches, one by studying the current helicity of the global Sun and the other by using the so-far most accurate vector magnetic field measurements provided with SP/Hinode. We present results using the first approach in Section 2 and results using the second approach in Section 3. We conclude and give a brief discussion in Section 4.

2.   Current helicity pattern of the global Sun

The data we used in this study (Wang & Zhang 2010) are full-disk longitudinal magnetograms obtained by three instruments. They are: the Michelson Doppler Imager (MDI) on board SOHO, the Kitt Peak Vacuum Telescope (KPVT) and the Synoptic Optical Long Term Investigations of the Sun (SOLIS) at Kitt Peak of the National Solar Observatory of the United States. We have used the same reconstruction technique in Pevtsov & Latushko (2000) to construct the vector magnetic field from longitudinal magnetograms. By assuming that the magnetic field evolves rather slowly and interpreting the variation of the observed B_{long} during a certain period of time as the result of changing position angles only, we can then use a set of observed B_{long} maps to reconstruct the synoptic maps of B_r, B_θ and B_ϕ.

Three time periods are studied as three representative phases of solar cycle 23. Two are selected during the solar minimums and one near the solar maximum. Of the two during solar minimum, one is in the ascending phase around September 1996 and one in the descending phase around June 2007. The one near the solar maximum is around August 2001.

For each time period, we first used the method in Pevtsov & Latushko (2000) to reconstruct the vector magnetic field of the global Sun. Note that here the vector magnetic fields obtained in this way are of highly-smoothed, with a width of smoothing window 5 - 15 degrees on the Sun. This results in a magnitude of a few Guass for the three components of the obtained fields. This magnitude is at least one magnitude
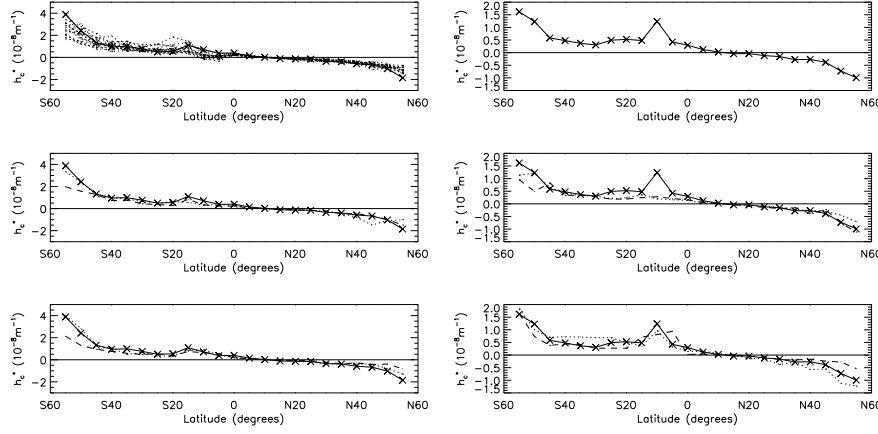
Figure 1. Profiles of normalized average current helicity (h_c^*) with the latitude. Left panels are those using MDI data and the right panels are of KPVT data. See text for detailed descriptions.

smaller than the sensitivities of current observations (transverse fields in particular) and makes this set of observations unique to study current helicity in large-scale magnetic fields.

Based on the obtained vector magnetogram, we then computed the current helicity density map by $h_c(\phi, \theta) = B_r(\nabla \times B)_r = \frac{1}{\sin\theta} \{ \frac{\partial}{\partial\theta}[\sin\theta B_\phi(\phi,\theta)] - \frac{\partial B_\theta(\phi,\theta)}{\partial\phi} \} B_r(\phi,\theta)$. We went on to get the profile of the latitudinal distribution of current helicity $h_c(\theta)$ by averaging the above $h_c(\phi, \theta)$ map over all longitudes of the same latitude and normalizing the profile using the averaged polaroid magnetic flux: $h_c^*(\theta) = \frac{h_c(\theta)}{\overline{B_r^2}}$. Here B_r is the reconstructed radial magnetic field and this normalization will eliminate the influence of the variation of magnetic flux with the solar cycle and will also reduce the influence of different calibrations between different instruments.

Figure 1 shows these normalized profiles of $h_c^*(\theta)$ obtained during the solar rotation starting on September 14, 1996. This is a time period during the solar minimum, at the beginning of solar cycle 23. Left panels are those obtained using MDI data and the right panels are of KPVT data. For the left panels, each solid line shows the profile obtained from the vector fields obtained using the first full-disk magnetograms of the 15 daily full-disk magnetograms of each day with $\triangle t$ = 5 days ($\triangle t$ is the time during which we assume the large-scale field does not change much) and $\triangle S$ = 184$''$ ($\triangle S$ is the size to which we reduce the spatial resolution to reflect the large-scale structure). Solid lines in right panels are the $h_c^*(\theta)$ profile obtained from the KPVT data. Dotted lines in the left-top panel are the $h_c^*(\theta)$ profiles obtained using other 14 full-disk magnetograms of each day, still with $\triangle t$ = 5 days and $\triangle S$ = 184$''$. We see here that, despite the different magnetograms and different instruments used, the obtained profile show

clearly hemispheric sign rule, that is, positive helicity sign in the southern hemisphere and negative helicity sign in the northern hemisphere, for all latitudes.

In the middle panels of Fig. 1 we plot the profiles of $h_c^*(\theta)$ obtained by changing $\triangle t$ values. The dotted lines show the profiles using $\triangle t$=3 days and the dashed lines for $\triangle t$=4 days, with $\triangle S$=184″. Again, we see that changing the $\triangle t$ values does not change the profile of $h_c^*(\theta)$ much. That means the existence of the evidences of the hemispheric sign rule is independent of the $\triangle t$ values we have used. Similarly, in the bottom panels of Fig.1 we plot the profiles of $h_c^*(\theta)$ obtained by changing $\triangle S$ values. Here the dotted lines show the profiles using $\triangle S$=90″ and the dashed lines show the profiles using $\triangle S$=224″, with $\triangle t$=5 days. Once again, we see that changing the $\triangle S$ values does not change the profile of $h_c^*(\theta)$ much and the existence of the evidences of the hemispheric sign rule is also independent of the $\triangle S$ values we have used.

Profiles at two other time periods give similar results. Our study shows that the large-scale magnetic fields show a clear and consistent current helicity pattern that follows the established hemispheric rule, that is, positive helicity sign in the southern hemisphere and negative helicity sign in the northern hemisphere. This hemispheric sign pattern is evident in the global magnetic field, extending to 60 degrees high in latitudes, in both solar minimum and maximum phases, and independent of the instruments and the parameters that we have used.

3.   Sunspot observation by SP/Hinode

Since its launch in September 2006, Hinode has provided us with high spatial-resolution vector magnetograms for both the descending phase of solar cycle 23 and the ascending phase of solar cycle 24. This gives us a unique chance to use these so-far most accurate vector magnetic field measurements to shed a light on the argument of solar-cycle dependence of hemispheric helicity sign rule.

In this study (Hao & Zhang 2011) we composed a sample of 64 active regions observed by SP/Hinode. This includes 30 active regions in solar cycle 23 and 34 active regions in solar cycle 24. We calculated two different helicity parameters, α_z and α_{hc}, for these 64 ARs. α_z is the mean value of local twist, defined as $\alpha_z = \overline{(\nabla \times \boldsymbol{B})_z / B_z}$. α_{hc} is the normalized mean current helicity density, obtained by $\alpha_{hc} = \frac{\sum (\nabla \times \boldsymbol{B})_z B_z}{\sum B_z^2}$. Both the averaging and integral are done over the whole magnetogram. In calculating α_z and α_{hc}, we have used two different representations of magnetic field measurement. One is related to "flux density", where the longitudinal magnetic field $B_z = f \cdot B \cos(\gamma)$ and the transverse magnetic field $B_t = \sqrt{f} \cdot B \sin(\gamma)$. The other is the "field strength" where $B_z = B \cos(\gamma)$ and $B_t = B \sin(\gamma)$. Hereafter we present the first type as B_z^1, B_t^1 and the second type as B_z^2, B_t^2. Correspondingly helicity parameters are also hereafter presented as α_z^1, α_{hc}^1 and α_z^2, α_{hc}^2 respectively.

Figure 2 presents the variation of α_z^1 (left panels) and α_z^2 (right panels) with the

solar latitude for the 30 ARs in the descending phase of solar cycle 23 (top panels), the 34 ARs in the ascending phase of solar cycle 24 (middle panels) and the total 64 ARs (bottom panels). Here α_z^1 and α_z^2 are calculated only using points with $|B_z^1| > 100$ G or $|B_z^2| > 100$ G . The solid lines indicate the results of least-square linear fits. Values of $d\alpha/d\theta$ from the linear fittings are also shown in Fig.2, in the unit of $10^{-9} m^{-1} deg^{-1}$. Here we see that for the 30 ARs of solar cycle 23, $d\alpha/d\theta$ for α_z^1 and α_z^2 are all positive. Out of these 30 ARs, only 8 (27%) ARs of the α_z^1 obey the usual hemisphere sign rule. This means that ARs in the descending phase of solar cycle 23 do not follow the usual hemispheric helicity sign rule.

Contrary to that in solar cycle 23, for the 34 ARs of solar cycle 24, 20 (59%) ARs of the α_z^1 obey the usual hemisphere sign rule. $d\alpha/d\theta$ for α_z^1 and α_z^2 are all negative. This means that ARs in the ascending phase of solar cycle 24 follow the usual hemispheric helicity sign rule, contrary to the prediction made in Choudhuri et al. (2004). Note that ARs in the descending phase of solar cycle 23 do show a deviation from the usual hemispheric helicity sign rule. We speculate that the physical process described in Choudhuri et al. (2004), that is, poloidal flux lines getting wrapped around a toroidal flux tube rising through the convection zone to give rise to the helicity, may still apply, but a phase shift may be required in the dynamo model used.

For all of the 64 ARs, 28 (44%) ARs of the α_z^1 follow the usual hemisphere sign rule. As a whole, these 64 ARs still follow the usual hemispheric helicity sign rule, with $d\alpha/d\theta$ for α_z^1 and α_z^2 all negative. This is consistent with the results from most previous studies, that is, most ARs follow the usual hemispheric helicity sign rule. Study on α_{hc}^1 and α_{hc}^2 gives similar results.

Despite for the fact that we have used the so-far most accurate measurement of vector magnetic field given by SP/Hinode, the hemispheric helicity sign rule observed is still weak with large scatters. As an evidence, we see from Fig. 2 that the magnitudes of the correlation coefficients between the latitude and the helicity parameters are all low, with the maximum magnitude only being 0.21. This seems indicating that the large scatter is an inherent property of the rule, not caused by the measurement errors. This is consistent with the prediction in Longcope, Fisher & Pevtsov (1998), where helicity is considered to be produced in the process of magnetic flux tubes rising through the solar convection zone and being buffeted by turbulence with a non-vanishing kinetic helicity ($\Sigma-$ effect).

Further analysis also shows that the inner umbra and outer penumbra has the opposite helicity sign. This seems consistent with the model of Chatterjee, Choudhuri & Petrovay (2006) where they model the penetration of a poloidal field into a toroidal rising flux tube through turbulence diffusion and predict the existence of a ring of reverse current helicity on the periphery of active regions.
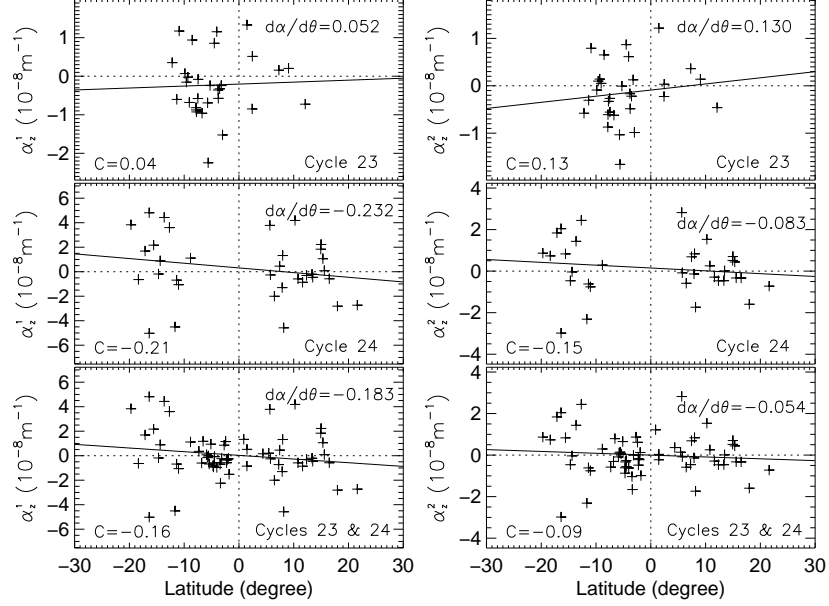
Figure 2. Variation of α_z^1 (left panels) and α_z^2 (right panels) with the solar latitude for the 30 ARs in solar cycle 23 (top panels), the 34 ARs in solar cycle 24 (middle panels) and the total 64 ARs (bottom panels). Shown also in the left-bottom corner of each panel are the correlation coefficients between latitude and α_z^1 or α_z^2.

4.   Conclusion and discussion

Our studies conclude that: (1) For large-scale magnetic field, hemispheric helicity sign rule presents in fields up to 60 degrees in latitude and shows no solar-cycle dependent. (2) For active regions observed by SP/Hinode, the usual hemispheric helicity sign rule is preserved in the ascending phase of solar cycle 24, but not in the descending phase of solar cycle 23.

Our observations seem consistent with the model by Longcope et al. (1998) and the model by Chatterjee et al. (2006). Results also seem suggesting that Choudhuri et al. (2004) has a merit in its physical picture, but may need to modify their result on which phase of the solar cycle that deviations from the hemispheric rule take place. From our observations we speculate that both the Σ-effect (Longcope et al. 1998) and the dynamo (Choudhuri et al. 2004; Chatterjee et al. 2006) have contributed in the generation of helicity, whereas in both models turbulence in the convection zone has played an important role.

Acknowledgements

References

Bao S. D., Zhang H. Q., 1998, ApJ, 496, L43
Bao S. D., Ai G. X., Zhang H. Q., 2000, JAA, 21, 303
Chatterjee P., Choudhuri A. R., Petrovay K., 2006, A&A, 449, 781
Choudhuri A. R., Chatterjee P., Nandy D., 2004, ApJ, 615, L57
Hagino M., Sakurai T., 2004, PASJ, 56, 831
Hagino M., Sakurai T., 2005, PASJ, 57, 481
Hao J., Zhang M., 2011, ApJ, 733, L27
Longcope D. W., Fisher G. H., Pevtsov A. A., 1998, ApJ, 507, 417
Pevtsov A. A., Canfield R. C., Metcalf T. R., 1995, ApJ, 440, L109
Pevtsov A. A., Canfield R. C., Latushko S. M., 2001, ApJ, 549, L261
Pevtsov A. A., Canfield R. C., Sakurai T., Hagino M. 2008, ApJ, 677, 719
Pevtsov A. A., Latushko S. M., 2000, ApJ, 528, 999
Tiwari S. K., Venkatakrishnan P., Sankarasubramanian K., 2009, ApJ, 702, L133
Wang C. Y., Zhang M., 2010, ApJ, 720, 632
Xu H., Gao, Y., Popova E. P., Nefedov S. N., Zhang H., Sokoloff D., 2009, ARep, 53, 160
Zhang M., 2006, ApJ, 646, L85
Zhang H., Sakurai T., Pevtsov A., Gao Y., Xu H., Sokoloff D., Kuzanyan K., 2010, MNRAS, 402, L30